

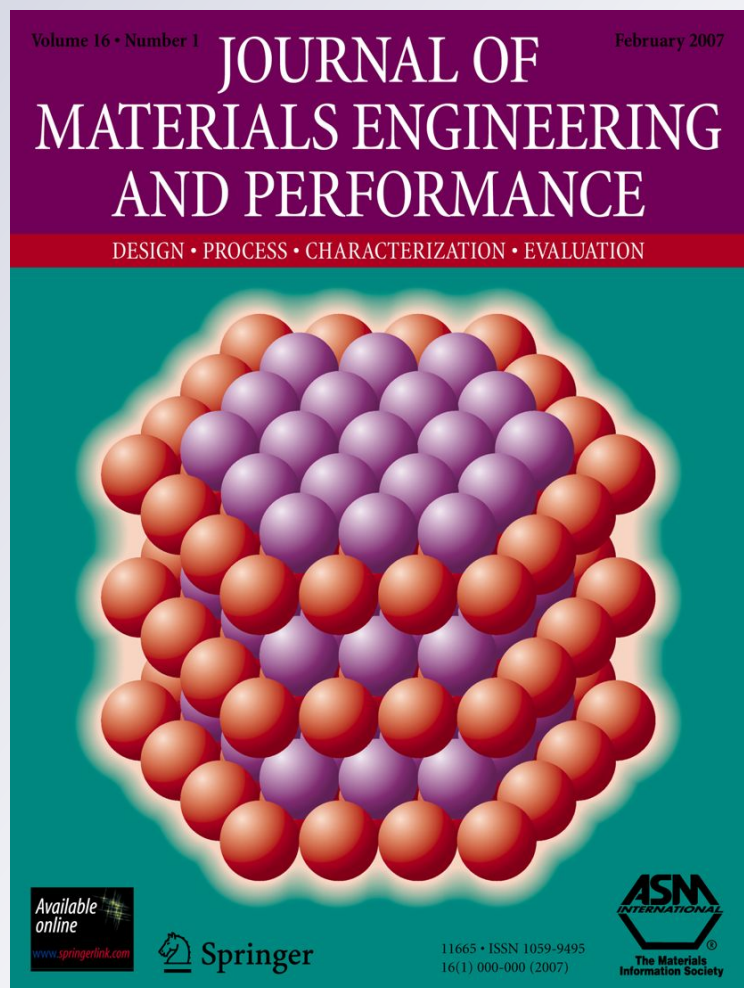
# *Comparison of Inclusions in Cold Drawn Wire and Precursor Hot-Rolled Rod Coil in VIM-VAR Nickel-Titanium Alloy*

**Frank Sczerzenie, Graeme Paul & Clarence Belden**

**Journal of Materials Engineering and Performance**

ISSN 1059-9495  
Volume 20  
Combined 4-5

J. of Materi Eng and Perform (2011)  
20:752-756  
DOI 10.1007/s11665-011-9832-4



 Springer

**Your article is protected by copyright and all rights are held exclusively by ASM International. This e-offprint is for personal use only and shall not be self-archived in electronic repositories. If you wish to self-archive your work, please use the accepted author's version for posting to your own website or your institution's repository. You may further deposit the accepted author's version on a funder's repository at a funder's request, provided it is not made publicly available until 12 months after publication.**

# Comparison of Inclusions in Cold Drawn Wire and Precursor Hot-Rolled Rod Coil in VIM-VAR Nickel-Titanium Alloy

Frank Sczerzenie, Graeme Paul, and Clarence Belden

(Submitted May 11, 2010; in revised form December 8, 2010)

Inclusion content is important for the mechanical behavior and performance of Nitinol wires, particularly in fatigue-rated devices. The purpose of this work was to make a quantitative comparison between inclusion populations in cold drawn wires and the precursor populations in hot-rolled rod coil. Inclusion content was examined in a series of VIM-VAR alloys with different transformation temperatures (TTR) controlled by the Ni to Ti ratio. This range of chemistry was chosen to assess the effect of Ni to Ti ratio on inclusion formation. In order to understand the differences in behavior between carbides and intermetallic oxides in wire drawing, carbides, and intermetallic oxide inclusions were measured separately using optical metallography pursuant to ASTM F2063. In VIM-VAR alloys at higher Ni to Ti ratios about 50.79 a/o Ni the formation of intermetallic oxides appears to be suppressed in the as-cast material through the presence of carbon and the precipitation of eutectic TiC in place of eutectic  $Ti_4Ni_2O_x$ . The structure of VIM-VAR alloy also varies after hot working depending on the TTR of the alloy. Higher TTR binary alloys with lower Ni to Ti ratios tend to have more and larger intermetallic oxides and fewer and smaller carbides after hot working. Microsegregation plays a role in inclusion formation. That is, during solidification, C, O, N diffuse to the interdendritic regions. This increases the potential for the precipitation of nonmetallic species. Carbides and intermetallic oxides behave differently in hot working and cold drawing. The change in maximum carbide size from coil to wire is very near zero for all Ni to Ti ratios. The change in maximum inclusion size from coil to wire is driven mainly by the fracture of intermetallic oxides and the formation of intermetallic oxide stringers.

**Keywords** biomaterials, cold drawing, electron microscopy, hot rolling, metallography, nitinol, quantitative

## 1. Introduction

Inclusion content is important for the mechanical behavior and performance of Nitinol wires, particularly in fatigue-rated devices. Current commercial specifications for Nitinol require the certification of inclusion content at a raw material dimension between 94 and 6.3 mm (Ref 1). For wire this is done on hot-rolled coil. Recently, Toro et al. compared the inclusion species in cold draw tubing made by different melting processes (Ref 2). They observed that tubing made from vacuum induction melted (VIM) alloy contained carbides (TiC). Tubing made from alloy that was vacuum arc re-melted after vacuum induction melting (VIM-VAR) contained both carbides and oxides ( $Ti_4Ni_2O_x$ ). Tubing made from VAR only

alloy contained only oxides. The quality of the VIM/VAR tubing was affected by the fragmentation of intermetallic oxides and the formation stringers of inclusions during tube drawing. The purpose of this work was to make a quantitative comparison between inclusion populations in cold drawn wires and the populations in the precursor hot-rolled coil in VIM-VAR alloy.

## 2. Experimental

Inclusion content was examined in a series of VIM-VAR alloys with different transformation temperatures (TTR) controlled by the Ni to Ti ratio. The alloys are designated by austenite start temperature,  $A_s$ , in the fully annealed condition (Ref 3). Alloys varied from  $A_s = -25$  °C (50.79 a/o Ni) to  $A_s = +95$  °C (49.63 a/o Ni). This range of chemistry was chosen to assess the effect of Ni to Ti ratio on inclusion formation in hot-rolled coil and cold drawn NiTi wire. In order to determine the differences in behavior between carbides and oxides in wire drawing, carbides and intermetallic oxide inclusions were measured separately. Seven alloy formulations were evaluated at 6.3-mm diameter hot-rolled coil and at 2.2 mm cold drawn wire taken from the same coil. Longitudinal centerline samples were polished in stages through 120 grit stone, 240 grit paper, 15  $\mu$ m diamond, 9  $\mu$ m diamond and finally 3  $\mu$ m diamond. The samples were examined at 500 diameters magnification on a Zeiss Observer DIM inverted

This article is an invited paper selected from presentations at Shape Memory and Superelastic Technologies 2010, held May 16-20, 2010, in Pacific Grove, California, and has been expanded from the original presentation.

Frank Sczerzenie, Graeme Paul, and Clarence Belden, SAES Smart Materials, New Hartford, NY. Contact e-mails: frank\_sczerzenie@saes-group.com and Graeme\_Paul@saes-group.com.

**Table 1 Carbides and intermetallic oxides in hot-rolled coil and cold drawn wire**

$A_s$ , °C	Coil maximum carbide		Coil minimum % fields Carbides <12.5 m	Coil maximum intermetallic		Coil maximum % fields Without intermetallic	Redraw maximum carbide		Redraw minimum % fields Carbides <12.5 m	Redraw maximum intermetallic		Redraw maximum % fields Without intermetallic
	µm	%		µm	%		µm	%		µm	%	
-25	15.62	0.95	77.8	16.16	1.04	100.0	18.51	1.00	88.9	87.09	1.38	100.0
0	15.12	0.70	66.7	11.08	0.27	100.0	12.10	0.96	88.9	34.46	0.44	100.0
30	13.25	1.08	77.8	24.10	0.84	22.2	13.42	0.72	88.9	49.22	0.74	77.8
55	6.58	0.66	100.0	17.22	0.68	0.0	7.23	0.53	100.0	27.71	0.63	0.0
70	10.59	0.71	100.0	17.13	0.77	0.0	8.65	0.82	100.0	110.95	1.52	0.0
95	10.98	0.46	100.0	31.01	2.94	0.0	12.32	0.67	100.0	107.94	2.80	0.0

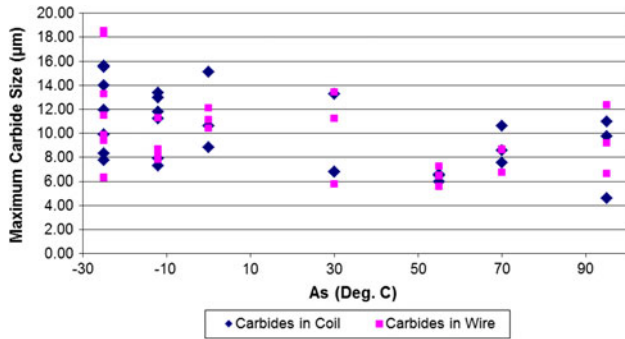


**Fig. 1** Maximum carbide size for coil and wire vs. TTR

stage metallograph in the as-polished condition. In this condition, carbides intermetallic oxides, voids, and matrix can be differentiated by color in the light microscope. Fracture and the separation of intermetallic oxide particles often created voids between oxide particles and between oxide and adjacent carbide particles in the cold drawn wire. No attempt was made to count void area separately from the oxide or carbide areas. The images were digitized, analyzed, and counted using the ImagePro3 analysis software.

### 3. Results

Table 1 shows the results in terms of the maxima for all samples at each TTR. Figures 1-4 show the maximum observed size and area fractions for the individual samples.

Maximum carbide size in coil ranged up to 16 µm. Maximum carbide size in wire ranged up to 19 µm. Maximum carbide size in wire is nominally the same as maximum carbide size in coil, Fig. 1. Maximum carbide size decreases slightly with decreasing Ni to Ti ratio. Maximum area fraction of carbides also tends to decrease with increasing TTR and decreasing Ni to Ti ratio, Fig. 2.

Maximum intermetallic oxide size in coil ranges up to 31 µm, Fig. 3. Maximum intermetallic oxide size in wire ranges up to 110 µm. Maximum intermetallic size in wire is increased due to fracture and the formation of stringers of the inclusions in linear arrays, Fig. 5. A hot-rolled coil structure is shown in Fig. 5(a). The cold drawn wire from the same coil is shown in Fig. 5(b). In the wire sample, the stringer is a

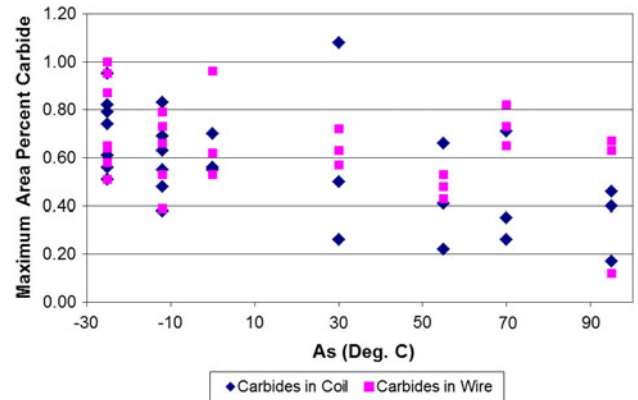


**Fig. 2** Maximum area fraction of carbides in coil and wire vs. TTR

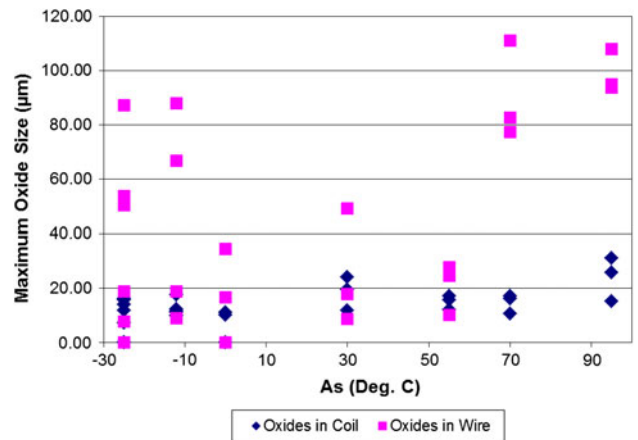


**Fig. 3** Maximum intermetallic size in coil and wire vs. TTR

combination of carbides and oxides. In the precursor coil there are several carbides enveloped in oxide. It can be surmised that a composite particle can fracture and form a stringer containing both oxide and carbide.

The maximum area of oxides was 2.94% at the highest TTR. However, maximum area fraction of intermetallic oxide does not increase monotonically with decreasing Ni to Ti ratio, Fig. 4. There appears to be a minimum at intermediate TTRs. This is discussed below.

## 4. Discussion

As-cast NiTi alloy structures depend on the trace element chemistry resulting from the melting process. Frenzel has shown that as-cast VIM alloy has carbides formed by reactions with the crucible (Ref 4). In the first instance, a TiC skull is formed at the crucible to melt interface. Particles of TiC from the skull can be entrained in the melt. In the second instance, Frenzel found that, at low carbon concentrations, TiC is not stable in liquid NiTi. Rather, carbides precipitate by a eutectic reaction during solidification (Ref 5). Zhang also showed that carbon dissolved in the melt precipitates as TiC by a eutectic reaction in the interdendritic zones (Ref 6).

In contrast, but in a similar solidification reaction, Moreira has shown that very low-carbon electron beam melted alloy has intermetallic oxides precipitated by a eutectic reaction in the interdendritic zones (Ref 7). In VIM-VAR alloy at 50.79 a/o Ni, the inclusions in as-cast ingot are carbides formed by a eutectic reaction in the last to freeze interdendritic liquid. This has been confirmed in ingots up to 406-mm diameter by scanning electron microscopy (SEM) of ingot samples using backscattered electron imaging (BEI). Figure 6 shows an interdendritic array of carbides. Intermetallic oxides are easily identified by differences in contrast in both cast and wrought alloy samples by SEM-BEI. There were no intermetallic oxides observed in

samples from the center, mid-radius or edge of the 406-mm diameter ingot. The carbides are found only in the interdendritic regions and the longest carbide is 53  $\mu\text{m}$ . Figure 7 is a

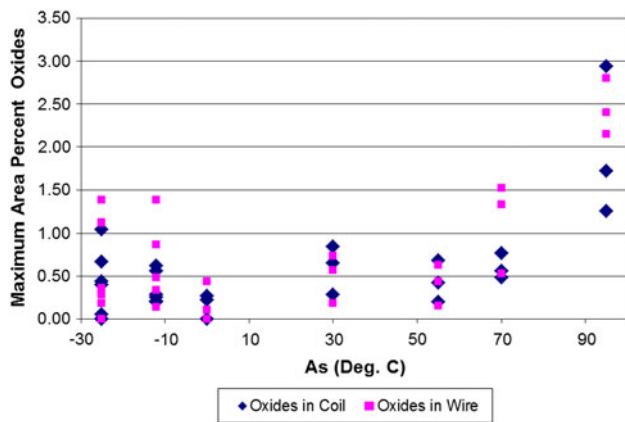


Fig. 4 Maximum area fraction of oxides in coil and wire vs. TTR

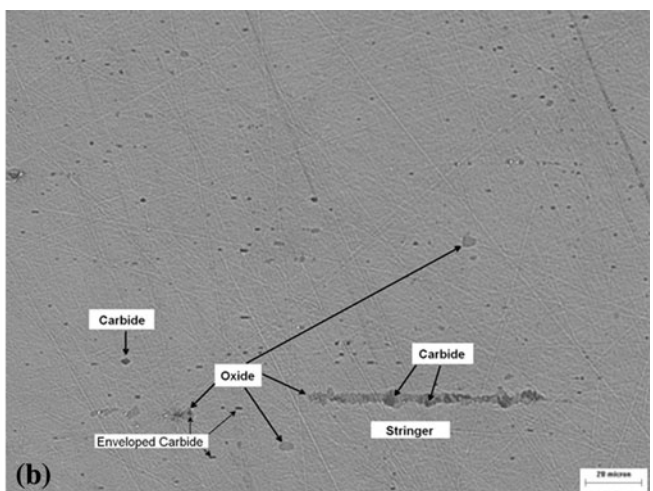
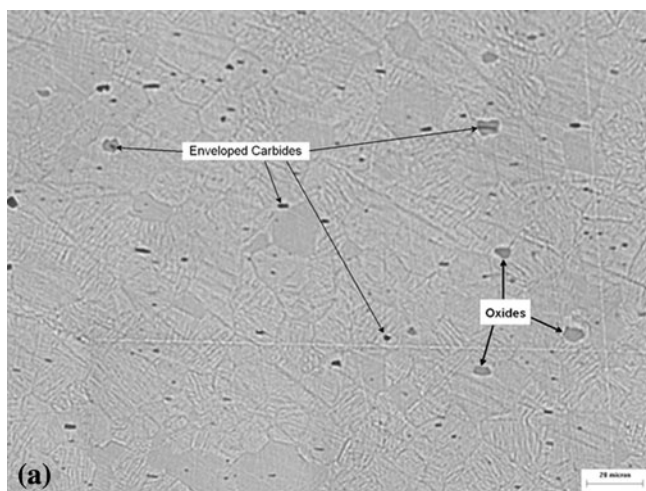


Fig. 5 (a) Hot-rolled coil, C5-9954-8T. (b) Cold drawn wire C5-9954-8-4

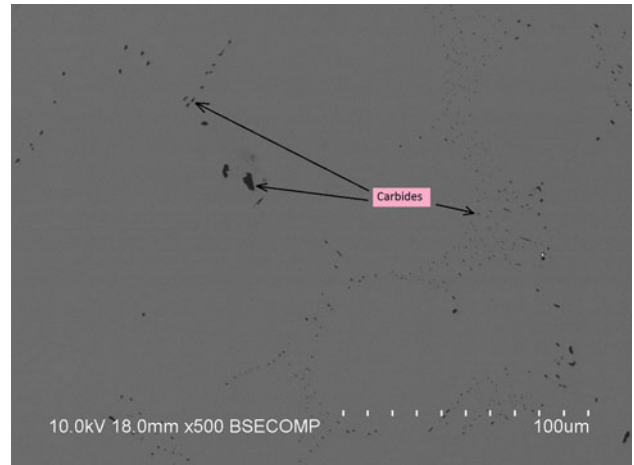


Fig. 6 As-cast VIM-VAR ingot, C5-9331

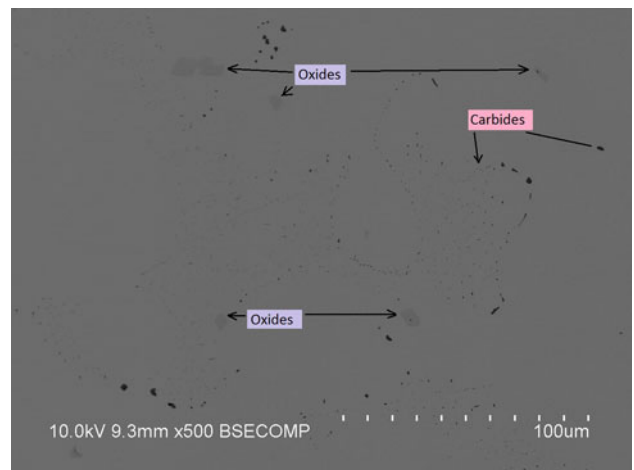


Fig. 7 As-cast NiTi ingot sample heat treated for  $8.64 \times 10^4$  s at 1000 °C, C5-9331

SEM-BEI image of a heat-treated ingot sample. This micrograph shows several large intermetallic oxide precipitates formed in the interdendritic regions of the sample heat treated at 1000 °C. Two of the oxides are formed around carbides. The interdendritic distribution of carbides and the subsequent interdendritic distribution of intermetallic oxides indicate that

microsegregation and small changes in local chemistry during solidification play a major role in inclusion formation.

The structure of VIM-VAR alloy varies after hot working depending on the TTR of the alloy, Fig. 8. At  $A_s = +55$  to  $+95$  °C, all coil and redraw samples had intermetallic oxides in all fields of view. At  $A_s = +30$  °C the percentage of fields with intermetallic oxides begins to drop. At  $A_s = -25$  to  $0$  °C, some coil and wire samples have no intermetallics. However, maximum intermetallic size and area fraction do not increase linearly with TTR. There appears to be a minimum in the intermetallic size at intermediate TTR. Also, the change in maximum intermetallic size after cold drawing is a minimum in the range of  $A_s = 0$  to  $+55$  °C. This leads to the hypothesis that intermediate TTRs are nearer to optimum chemistry for the VIM-VAR alloy and a minimum in the driving force for the formation of intermetallics oxides.

The change in maximum carbide size from coil to redraw is small for all TTRs, Fig. 2. This is consistent with the findings of Toro et al. that very few carbides are fractured during cold drawing. Maximum carbide size and area fraction in coil and wire tend to decrease with increasing TTR, Fig. 2 and 3. There were no intermetallic oxides found in three wires and no intermetallic oxides in the corresponding parent coil. There were no instances where intermetallics were found in wire but not the parent coil or in coil but not the corresponding wire. At the same time, the size, area fraction, and frequency of intermetallic oxides increased with increasing TTR. Several observations were made of carbides encased in intermetallic oxide, Fig. 4, 9, and 10. Maximum carbide size and area fraction decrease in  $A_s = +55$  °C and warmer alloys. Since the changes in ingot chemistry are small, this phenomenon suggests that microsegregation plays a major role in inclusion formation. That is, during solidification, C, O, and N diffuse to the interdendritic regions. This increases the chemical potential for the precipitation of nonmetallic species.

#### 4.1 Optimum Processing

Figure 4 showed the structure of hot-rolled coil and wire made by standard processes. Cold drawing increased the maximum observed inclusion size from 8  $\mu\text{m}$  in the coil to 85  $\mu\text{m}$  in the wire. Subsequently, manufacturing processes

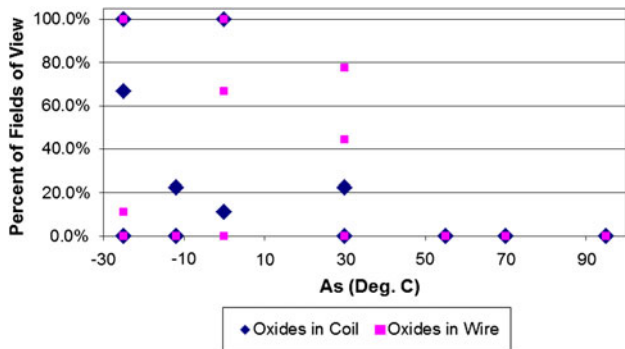


Fig. 8 Percent fields of view without intermetallic vs. TTR

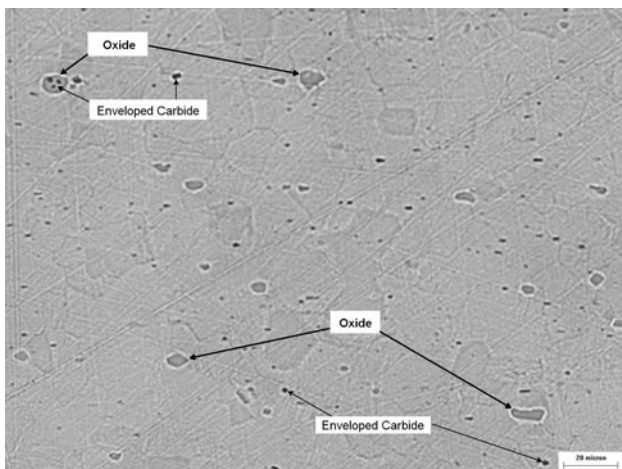


Fig. 9 Carbide enveloped in oxide in hot-rolled coil, C5-9923-T

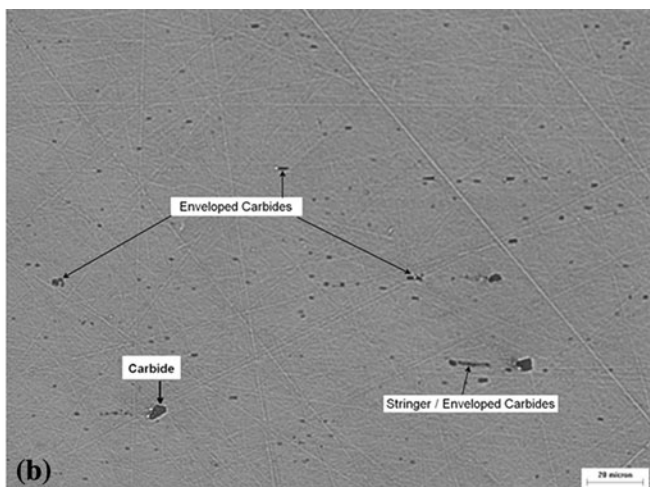
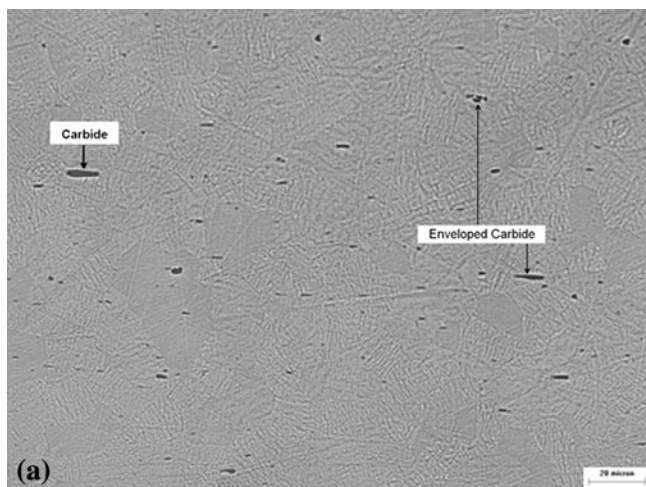


Fig. 10 (a) Hot-rolled coil from modified processing; carbides 13.77  $\mu\text{m}$  maximum, no intermetallic oxide, C9-8524-3. (b). Cold drawn wire from modified processing, 12.52  $\mu\text{m}$  maximum carbide, no intermetallic oxide, C9-8524-3

were modified to minimize the formation of intermetallic oxides, Fig. 10 shows the results in the coil and the wire. There were no isolated intermetallic oxides found in the hot-rolled coil or the wire. Small stringers of carbides enveloped in oxide were found in the cold drawn wire. Maximum carbide and stringer size is about 14  $\mu\text{m}$ .

## 5. Conclusions

Maximum inclusion size was compared in VIM-VAR hot-rolled coil and cold drawn wire made from the same coil by optical metallography pursuant to F2063. Carbide and intermetallic oxide populations were measured separately and compared for different Ni to Ti ratios.

Carbides and intermetallic oxides behave differently in hot working and cold drawing.

In as-cast VIM-VAR alloy at 50.79 a/o Ni the formation of intermetallic oxides appears to be suppressed through the presence of carbon and the precipitation of TiC.

The change in maximum inclusion size from coil to wire is driven mainly by the fracture of intermetallic oxides and stringer formation. Carbide stringers are very limited.

Higher TTR binary alloys with lower Ni to Ti ratios tend to have more and larger intermetallic oxides and fewer and smaller carbides after hot working.

This study was aimed at developing technology to provide NiTi alloy with reduced inclusion size and area fraction. This was achieved in production by controlling the entire manufacturing process from VIM through hot rolling. Intermetallic oxides and stringer formation were minimized in coil and wire.

## References

1. "ASTM International, Designation: F2063-05," *Standard Specification for Wrought Nickel-Titanium Shape Memory Alloys for Medical Devices and Surgical Implants*, ASTM Intl., West Conshohocken, PA, 2005
2. A. Toro, F. Zhou, M.H. Wu, W. Van Geertruyden, and W.Z. Mislolek, Characterization of Non-Metallic Inclusions in Superelastic NiTi Tubes, *J. Mater. Eng. Perform.*, 2009, **18**(5–6), p 448–458
3. "ASTM International, Designation: F2004-05," *Standard Test Method for Transformation Temperature of Nickel-Titanium Alloys by Thermal Analysis*, ASTM Intl., West Conshohocken, PA, 2005
4. J. Frenzel, K. Neuking, and G. Eggler, Induction Melting of NiTi Shape Memory Alloys—The Influence of the Commercial Crucible Graphite on Alloy Quality, *Mat.-wiss. u. Werkstofftech.*, 2004, **35**(5), p 352–358
5. J. Frenzel, K. Neuking, G. Eggler, and C. Haaberland, On the Role of Carbon During Processing of NiTi Shape Memory Alloys. *Proceedings SMST*, B. Berg, et al., ed., 2007, p 131–138
6. Z. Zang et al., On the Reaction Between NiTi Melts and Crucible Graphite During Vacuum Induction Melting of NiTi Shape Memory Alloys, *Acta Mater.*, 2005, **53**, p 3971–3985
7. C.T.A. Moreira, et al., Corrosion Behavior of Equiatomic NiTi SMA in Sodium Chloride Solution, *17th CBECIMat*, Novembro, 2006, Foz do Iguacu, Brasil, p 5124–5134